ALLEN, F. H. (1980). *Acta Cryst.* B**36**, 81–96.

AMMON, H. L., SHERRER, C. & AGRANAT, I. (1977). *Chem. Scr.* **11**, 39–43.

BECKER, P. J. & COPPENS, P. (1975). *Acta Cryst.* A**31**, 417–425.

BUSING, W. R., MARTIN, K. O. & LEVY, H. A. (1973). *J. Appl. Cryst.* **6**, 309–346.

DESIDERATO, R. & SASS, R. L. (1965). *Acta Cryst.* **18**, 1–4.

DIETRICH, H. (1970). *Acta Cryst.* B**26**, 44–55.

Enraf–Nonius (1982). *Enraf–Nonius CAD-4 Operation Manual.* Enraf–Nonius, Delft.

FILHOL, A. & THOMAS, M. (1984). *Acta Cryst.* B**40**, 44–59.

HERBSTEIN, F. H. (1971). *Perspectives in Structural Chemistry* IV, edited by J. D. DUNITZ & J. A. IBERS, pp. 166–395. New York: Wiley.

International Tables for X-ray Crystallography (1974). Vol. IV. Birmingham: Kynoch Press. (Present distributor D. Reidel, Dordrecht.)

JAUD, J., CHASSEAU, D., GAULTIER, J. & HAUW, C. (1974). *C. R. Acad. Sci.* **278**, 769–771.

JOHNSON, C. K. (1976). *ORTEP*II. Report ORNL-5138. Oak Ridge National Laboratory, Tennessee, USA.

KELLER, H. J. (1975). Editor. *Low-Dimensional Cooperative Phenomena.* New York: Plenum.

KISTENMACHER, T. J., PHILLIPS, T. E. & COWAN, D. O. (1974). *Acta Cryst.* B**30**, 763–768.

KOPTSIK, V. A. (1966). *Shubnikov Groups.* Moscow State Univ. Press.

LELY, J. A. & BIJVOET, J. M. (1944). *Recl Trav. Chim. Pays-Bas,* **63**, 39–43.

LISSALDE, F., ABRAHAMS, S. C. & BERNSTEIN, J. L. (1978). *J. Appl. Cryst.* **11**, 31–34.

LUNDGREN, J.-O. (1982). Crystallographic computer program. Report No. UUIC-BB-4-05. Univ. of Uppsala, Sweden.

MCCOY, B. M. & WU, T. T. (1973). *The Two-Dimensional Ising Model.* Harvard Univ. Press.

MAIN, P., HULL, S. E., LESSINGER, L., GERMAIN, G., DECLERCQ, J.-P. & WOOLFSON, M. M. (1978). *MULTAN78. A System of Computer Programs for the Automatic Solution of Crystal Structures from X-ray Diffraction Data.* Univs. of York, England, and Louvain, Belgium.

MILLER, J. S. & EPSTEIN, A. J. (1978). Editors. *Synthesis and Properties of Low-Dimensional Materials.* New York Academy of Sciences.

MORTENSEN, M. (1982). *Phys. Scr.* **25**, 854–856.

PARKES, A. S. & HUGHES, R. E. (1963). *Acta Cryst.* **16**, 734–736.

PAULING, L. (1960). *The Nature of the Chemical Bond,* 3rd ed. Ithaca: Cornell Univ. Press.

POUGET, J. P., SHIRANE, G., BECHGAARD, K. & FABRE, J. M. (1983). *Phys. Rev. B,* **27**, 5203–5206.

RINDORF, G., SOLING, H. & THORUP, N. (1982). *Acta Cryst.* B**38**, 2805–2808.

SOOS, Z. G. (1974). *Annu. Rev. Phys. Chem.* **25**, 121–153.

SUNDARALINGAM, M. & JENSEN, L. H. (1966). *J. Am. Chem. Soc.* **88**, 198–204.

SUTTON, L. E. (1965). *Tables of Interatomic Distances and Configuration in Molecules and Ions. Supplement.* Spec. Publ. No. 18. London: The Chemical Society.

WARD, M. D. (1987). *Organometallics,* **6**, 754–762.

Acta Cryst. (1988). B**44**, 271–281

Thermal Vibrations and Electrostatic Properties of Parabanic Acid at 123 and 298 K

BY X. M. HE,* S. SWAMINATHAN AND B. M. CRAVEN†

Department of Crystallography, University of Pittsburgh, Pittsburgh, PA 15260, *USA*

AND R. K. MCMULLAN

Chemistry Department, Brookhaven National Laboratory, Upton, NY 11973, *USA*

(*Received* 8 *June* 1987; *accepted* 4 *November* 1987)

Abstract

The crystal structure of parabanic acid ($1H,3H$-imidazoletrione, $C_3H_2N_2O_3$, $M_r = 114{\cdot}1$) at 123 K [monoclinic, $P2_1/n$, $Z = 4$, $a = 10{\cdot}704\,(2)$, $b = 8{\cdot}187\,(2)$, $c = 4{\cdot}969\,(1)$ Å, $\beta = 92{\cdot}32\,(1)°$] has been determined by neutron and X-ray diffraction. Neutron reflections [1658, $(\sin\theta)/\lambda \le 0{\cdot}78$ Å^{-1}, $\lambda = 1{\cdot}0470\,(1)$ Å, $\mu = 0{\cdot}75$ cm^{-1}] in full-matrix least-squares refinement ($wR = 0{\cdot}055$) gave nuclear parameters with bond lengths having estimated standard deviations (e.s.d.'s) of 0·001 Å. X-ray reflections [3150 with $|F| \ge 3\sigma$ and $(\sin\theta)/\lambda \le 1{\cdot}3$ Å^{-1}, Mo $K\alpha$, $\lambda = 0{\cdot}7093\,(1)$ Å, $\mu = 1{\cdot}708$ cm^{-1}] were used in full-matrix least-squares refinement ($R = 0{\cdot}022$) assuming Stewart's rigid pseudoatom model, so as to determine the charge-density distribution. Sharp features near the O nuclei in the residual electron density map noted by Craven & McMullan (CM) [*Acta Cryst.* (1979), B**35**, 934–945] in their 298 K study were absent at 123 K. New refinements using CM's 298 K data give significant third-order thermal parameters for O atoms due to anharmonic molecular stretching, with good agreement between probability density functions, (p.d.f.'s) from X-ray and neutron diffraction. When deconvoluted from the thermal vibrations in the crystal, deformation charge densities derived at 298 and 123 K are in satisfactory agreement and conform closely to the $2mm$ symmetry of the isolated molecule. The molecular dipole moment is 2·3 (3) D [$7{\cdot}7\,(10) \times 10^{-30}$ C m]. A map of molecular electrostatic potential indicates that

---

* Present address: Department of Biology, University of Utah, Salt Lake City, UT 84112, USA.

† To whom correspondence should be addressed.

0108-7681/88/030271-11$03.00

the carbonyl O atoms in parabanic acid are weakly electronegative. This is confirmed by calculation of the electrostatic energy of interaction for the two distinct H-bonded pairs of molecules isolated from the crystal. Energy values are weakly attractive [−7 (3) and 5 (2) kJ mol^{-1}]. Similar calculations are less reliable for pairs of molecules forming intermolecular C···O distances as short as 2·75 Å. However, depending on the model, energy values are repulsive or negligibly small. Thus the high stability of parabanic acid crystals (m.p. 516 K with decomposition) cannot be explained.

Introduction

For determining the electrostatic properties of molecules from Bragg diffraction data, it is desirable that the static charge-density distribution should be properly deconvoluted from the atomic thermal vibrations in the crystal. If this has been done successfully, then diffraction data collected at different temperatures should give rise to the same static charge-density distribution. Also, since the nuclear positional and thermal parameters need to be determined without bias due to the effects of the electron density, it is desirable that neutron as well as X-ray diffraction data should be collected. If adequate models are assumed for the charge distribution and the thermal motion in the crystal, then there should be good agreement between atomic thermal parameters derived from X-ray and neutron diffraction. We report studies of parabanic acid (Fig. 1) at 123 and 298 K by X-ray and neutron diffraction in which these criteria are reasonably well satisfied.

The crystal structure of parabanic acid (Davies & Blum, 1955) is one of several with unusually short (<3 Å) intermolecular distances O=C···O involving carbonyl groups. They have been reviewed by Bolton (1964), Pullman (1964), Prout & Wallwork (1966) and Bürgi, Dunitz & Shefter (1974). From X-ray and neutron data for alloxan at 123 K, Swaminathan, Craven & McMullan (1985) concluded that the short C···O distances (2·73 Å) were associated with a depletion of electronic charge from the C atom along the direction of close C···O approach. In parabanic acid at 298 K, a similar charge depletion was reported (Craven & McMullan, 1979; hereafter CM), although in this structure there were features in the charge density close to the O nuclei which might also be implicated in the O=C···O interactions. These features could be interpreted as a polarization of the electron density in the O atomic core along the O···C direction. Alternatively, CM pointed out that they might arise from anharmonic thermal vibrations of the O atoms, or from some combination of both effects.

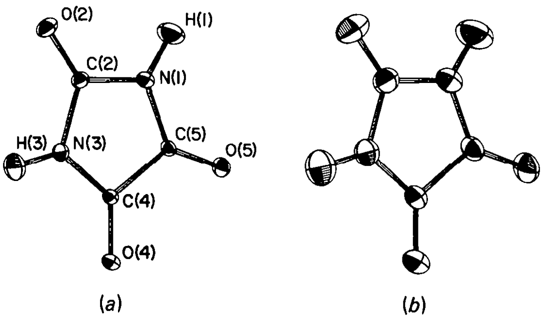

Fig. 1. Parabanic acid, showing atomic nomenclature and 50% probability thermal ellipsoids (Johnson, 1976) obtained from neutron diffraction, (a) at 123 K and (b) at 298 K.

In order to achieve a better deconvolution of the static charge distribution from the thermal vibrations, the crystal structure of parabanic acid has been redetermined from new low-temperature (123 K) X-ray and neutron data. We find that the sharp features at 298 K are due to thermal vibrations, since they are absent at 123 K. With this knowledge, new refinements with the CM data (298 K) are reported. The results at each temperature are self-consistent and there is also agreement between the two static charge-density distributions.

Experimental

(i) *Neutron diffraction at* 123 K

Neutron diffraction data collection at Brookhaven High Flux Beam Reactor followed procedures of Weber, Craven & McMullan (1983). Wavelength [λ = 1·0470 (1) Å] from least-squares fit of $\sin^2\theta$ data for KBr (a = 6·6000 Å at 298 K). Crystal of parabanic acid (volume 1·78 mm^3), same as used by CM, enclosed in Al cryostat cooled to 123 K by closed-cycle refrigerator.* Cell parameters from $\sin^2\theta$ for 32 reflections ($45 < 2\theta < 57°$). Intensities collected in one quadrant from $\omega/2\theta$ step scans, fixed width ($\Delta 2\theta = 2·8°$) for $(\sin\theta)/\lambda < 0·44$ Å^{-1} and variable width $\Delta 2\theta = (1·93 + 2·62 \tan\theta)°$ for $(\sin\theta)/\lambda < 0·78$ Å^{-1}. Background taken as first and last tenths of scan. Variance $\sigma^2(I) = I + 5B$. h −16–16, k 0–12, l 0–7. Absorption corrections by analytical procedure (de Meulenaer & Tompa, 1965; Templeton & Templeton, 1973), assuming mass absorption 2390 mm^2 g^{-1} for bound H (McMullan & Koetzle, 1979). With averaging of intensities in the $hk0$ zone [$R(F^2) = 0·011$], 1658 non-symmetry-related reflections obtained. Structure refinement by full-matrix least squares [locally modified program of Busing, Martin & Levy (1962)] to minimize $\sum(w\Delta^2)$ where $\Delta = F^2_{\rm obs} - F^2_{\rm cal}$ and $w = \{[\sin 2\theta\, \sigma(I)]^2 + (0·01F^2)^2\}^{-1}$. Coherent neutron scattering lengths from Koester (1977) and initial parameters values from CM. Variables were scale factor, isotropic extinction parameter g [type I crystal, Lorentzian mosaicity; Becker &

---

* Air Products and Chemicals, Inc., Displex Model CS-202.

Table 1. *Nuclear positional parameters* (×10⁵) *at* 123 K (*above*) *and* 298 K (*below*) *determined by neutron diffraction*

	x	y	z
N1	18916 (4)	32377 (6)	46675 (11)
	19439 (18)	32746 (19)	46590 (32)
C2	29385 (6)	36709 (9)	32563 (15)
	29856 (17)	36806 (25)	32964 (45)
O2	29520 (9)	44920 (11)	12468 (18)
	30001 (24)	45095 (33)	13242 (60)
N3	39750 (5)	29587 (7)	45863 (11)
	40126 (18)	29454 (19)	45651 (33)
C4	36357 (6)	20928 (9)	67736 (14)
	36700 (16)	20826 (25)	67093 (42)
O4	42889 (7)	13356 (12)	83826 (20)
	43152 (21)	13087 (35)	82601 (57)
C5	22009 (6)	22782 (8)	68214 (14)
	22419 (16)	23105 (24)	67655 (41)
O5	15313 (7)	16853 (11)	84723 (18)
	15703 (21)	17390 (31)	83793 (51)
H1	10019 (15)	35953 (23)	41066 (38)
	10574 (53)	36728 (59)	41195 (98)
H3	48752 (14)	30949 (23)	39595 (37)
	49102 (55)	30500 (56)	39402 (95)

Coppens (1974)], nuclear positional and anisotropic thermal parameters, totalling 92.* Convergence at $wR(F^2) = 0{\cdot}055$, $S = 1{\cdot}11$,† $g = 0{\cdot}70\,(2) \times 10^{-4}$ rad⁻¹. The most significant extinction corrections were $0{\cdot}45F^2_{\text{cal}}$ for 020 and 200. $\Delta/\sigma < 0{\cdot}01$. Final nuclear parameters (CM atomic nomenclature) are in Tables 1, 2 and 3.‡ Anisotropic thermal vibrational ellipsoids are shown in Fig. 1.

Table 2. *Anisotropic thermal parameters* (Å × 10⁴)

From above to below, values are from neutron and X-ray diffraction at 123 K, then from neutron and X-ray diffraction at 298 K. X-ray values were not obtained for H atoms. Temperature factors have the form

$$T = \exp[-2\pi^2 \textstyle\sum_i \sum_j h_i h_j a_i^* a_j^* U_{ij}].$$

	U_{11}	U_{22}	U_{33}	U_{12}	U_{13}	U_{23}
N1	88 (2)	124 (2)	124 (2)	15 (2)	−6 (2)	14 (2)
	79 (1)	126 (1)	132 (1)	17 (1)	−5 (1)	14 (1)
	185 (4)	277 (3)	295 (3)	44 (2)	−9 (2)	23 (2)
	178 (2)	280 (3)	288 (3)	47 (2)	−8 (2)	28 (3)
C2	118 (3)	107 (3)	95 (3)	1 (2)	1 (2)	14 (2)
	114 (1)	111 (1)	106 (1)	3 (1)	3 (1)	19 (1)
	261 (13)	242 (4)	236 (4)	8 (3)	12 (3)	27 (3)
	264 (2)	247 (3)	227 (3)	8 (2)	13 (2)	42 (2)
O2	206 (4)	150 (4)	115 (4)	−10 (3)	6 (3)	43 (3)
	205 (1)	153 (1)	132 (1)	−4 (1)	2 (1)	45 (1)
	475 (6)	363 (5)	319 (5)	2 (4)	17 (4)	119 (5)
	466 (5)	360 (5)	315 (4)	4 (4)	17 (1)	120 (4)
N3	90 (2)	151 (2)	135 (2)	−1 (2)	21 (2)	33 (2)
	80 (1)	155 (1)	142 (1)	3 (1)	24 (1)	37 (1)
	180 (4)	351 (3)	331 (3)	3 (2)	60 (2)	82 (3)
	179 (2)	360 (3)	311 (3)	11 (2)	69 (2)	91 (3)
C4	75 (2)	124 (3)	109 (3)	3 (2)	1 (2)	23 (2)
	67 (1)	127 (1)	121 (1)	4 (1)	−2 (1)	27 (1)
	141 (3)	301 (4)	285 (4)	5 (3)	10 (3)	63 (3)
	139 (2)	308 (3)	262 (3)	9 (2)	1 (2)	71 (2)
O4	90 (3)	186 (4)	176 (4)	−1 (3)	−23 (3)	62 (3)
	86 (1)	193 (1)	193 (2)	1 (1)	−27 (1)	74 (1)
	196 (4)	475 (6)	451 (6)	−1 (4)	−52 (4)	198 (5)
	182 (3)	484 (5)	440 (5)	−5 (3)	−54 (3)	207 (4)
C5	68 (2)	115 (3)	96 (3)	3 (2)	8 (2)	2 (2)
	66 (1)	115 (1)	104 (1)	1 (1)	10 (1)	5 (1)
	150 (3)	272 (3)	229 (3)	5 (2)	26 (2)	−2 (3)
	145 (2)	268 (2)	221 (2)	3 (2)	32 (2)	2 (2)
O5	99 (2)	179 (4)	121 (4)	−5 (3)	31 (2)	13 (2)
	88 (1)	180 (1)	136 (1)	−7 (1)	33 (1)	16 (1)
	202 (3)	423 (5)	310 (5)	−13 (3)	85 (3)	33 (4)
	190 (2)	426 (4)	309 (4)	−4 (3)	81 (3)	27 (4)
H1	165 (6)	339 (9)	277 (8)	69 (6)	−21 (5)	54 (7)
	276 (11)	570 (11)	537 (11)	137 (8)	−26 (8)	91 (9)
H3	159 (6)	326 (8)	238 (8)	−21 (7)	66 (5)	50 (7)
	292 (11)	564 (11)	523 (10)	−17 (7)	132 (8)	99 (9)

(ii) *X-ray diffraction at* 123 K

X-ray data collection with an Enraf–Nonius CAD-4 diffractometer using Nb-filtered Mo $K\alpha$ radiation. Cooling to 123 (2) K by N_2 gas stream from Enraf–Nonius device. Data collection with two crystals, large (0·22 × 0·24 × 0·32 mm) and small (0·02 × 0·10 × 0·38 mm), both from aqueous acetone, cleaved and fractured to avoid (001) twinning (see CM); mounted with longest dimension, c, close to diffractometer φ axis. Unit-cell parameters from $\sin^2\theta$ least-squares fit, 52 reflections ($19 < \theta < 24°$) measured at $\pm\theta$ [effective $\lambda = 0{\cdot}7093\,(1)$ Å from similar measurements on NaCl at 293 K assuming $a = 5{\cdot}6402$ Å]. Values $a = 10{\cdot}698\,(2)$, $b = 8{\cdot}182\,(2)$, $c = 4{\cdot}969\,(1)$ Å, $\beta = 92{\cdot}34\,(2)°$ agree with those from neutron diffraction (*Abstract*); latter used throughout. Intensity profiles from 48 points in $\omega/2\theta$ scan; total 5772 reflections large crystal, $(\sin\theta)/\lambda < 1{\cdot}3$ Å⁻¹; 1124 reflections small crystal, $(\sin\theta)/\lambda < 0{\cdot}6$ Å⁻¹; h −23–27, k 0–21, l 0–11. For $(\sin\theta)/\lambda > 1{\cdot}0$ Å⁻¹, measured only reflections $|E_{hkl}| > 2{\cdot}0$ predicted from neutron results. Three monitor reflections measured every 60 min. Lehmann & Larsen (1974) method of profile analysis, neglecting scan points below Nb absorption edge; Nelmes (1975) method for reflections $\theta < 5°$. For 333 weak reflections, peak windows assumed from neighboring strong reflections. X-ray absorption corrections ($\mu = 1{\cdot}708$ cm⁻¹) and crystal mean path lengths by Busing & Levy (1957) method. Variances $\sigma^2(I) = \sigma^2_{\text{counts}} + (pI)^2$ with $p = 0{\cdot}0056$ (large crystal), $p = 0{\cdot}0081$ (small crystal); p from monitor intensities (McCandlish, Stout & Andrews, 1975). In merged data (3150 reflections, $F_o > 3\sigma$), $p = 0{\cdot}015$ allowing for variance in interset scaling factor (He, 1984).

(iii) *Refinements with* 123 K *X-ray data*

Full-matrix least-squares structure refinements, computer program by Craven & Weber (1981), to minimize $\sum(w\Delta^2)$ where $\Delta = |F_{\text{obs}}| - |F_{\text{cal}}|$, $w = \sigma(F_{\text{obs}})^{-2}$. Seven different refinements were all based on rigid pseudoatom model (Stewart, 1976). Pseudoatoms assumed

---

* Refinement with third-order thermal parameters was also carried out (He, 1984), but none of the c_{jkl} values was significantly different from zero.

† $wR(F^2) = [\sum(w\Delta^2)/\sum(wF^4)]^{1/2}$; $S = \{[\sum(w\Delta^2)]/(m-n)\}^{1/2}$, $\Delta = F^2_{\text{obs}} - F^2_{\text{cal}}$.

‡ Lists of X-ray and neutron structure factors (123 K), third-order thermal parameters (from X-ray and neutron refinements at 298 K) and bond lengths and angles with thermal vibration corrections (from neutron diffraction at 123 and 298 K) have been deposited with the British Library Document Supply Centre as Supplementary Publication No. SUP 44583 (46 pp.). Copies may be obtained through The Executive Secretary, International Union of Crystallography, 5 Abbey Square, Chester CH1 2HU, England.

Table 3. *Electron population parameters* (× 100)

These are normalized values for the charge deformation terms referred to the crystal axes *a, b, c** (Epstein, Ruble & Craven, 1982). Slater-type radial functions have fixed exponents 8·50, 7·37, 6·50, 4·69 Å^{-1} for O, N, C and H pseudoatoms. Values obtained at 123 K are listed above those obtained at 298 K.

	p_v	d_1	d_2	d_3	q_1	q_2	q_3	q_4	q_5	o_1	o_2	o_3	o_4	o_5	o_6	o_7
N1	11 (2)	1 (1)	−3 (1)	−2 (1)	2 (1)	−2 (1)	2 (1)	2 (1)	−3 (1)	−2 (1)	9 (1)	−10 (1)	−2 (1)	4 (1)	−5 (1)	8 (1)
	10 (2)	−2 (1)	−2 (1)	−3 (1)	4 (1)	−5 (1)	3 (1)	−3 (1)	−3 (1)	0 (1)	10 (1)	−20 (2)	−1 (2)	7 (1)	−9 (2)	5 (2)
C2	−2 (2)	3 (1)	7 (1)	−7 (1)	5 (1)	−1 (1)	0 (1)	−25 (1)	8 (1)	−3 (1)	−12 (1)	20 (1)	−4 (1)	1 (1)	10 (1)	−13 (1)
	−4 (2)	0 (1)	12 (1)	−8 (1)	5 (1)	−2 (1)	−3 (1)	−27 (1)	10 (1)	−8 (1)	−11 (1)	19 (2)	−6 (2)	0 (1)	5 (1)	−15 (2)
O2	0 (1)	−1 (1)	5 (1)	−4 (1)	9 (1)	−2 (1)	1 (1)	−2 (1)	−5 (1)	0 (1)	1 (1)	0 (1)	1 (1)	0 (1)	−2 (1)	1 (1)
	6 (2)	3 (1)	8 (1)	−7 (1)	16 (2)	−4 (2)	−1 (1)	−5 (2)	−11 (1)	−3 (2)	−3 (2)	2 (1)	5 (1)	−3 (2)	−1 (2)	1 (2)
N3	9 (2)	−1 (1)	−1 (1)	1 (1)	3 (1)	−1 (1)	−3 (1)	0 (1)	−2 (1)	6 (1)	5 (1)	−12 (2)	6 (1)	−5 (1)	−4 (1)	10 (1)
	7 (2)	−4 (1)	−2 (1)	1 (1)	3 (1)	−3 (1)	−5 (1)	−2 (1)	0 (1)	9 (1)	8 (1)	−11 (1)	5 (2)	−7 (1)	−3 (2)	14 (2)
C4	12 (2)	1 (1)	−1 (1)	3 (1)	9 (1)	−10 (1)	9 (1)	−20 (1)	1 (1)	−14 (1)	0 (1)	5 (1)	−13 (1)	17 (1)	4 (1)	−6 (1)
	8 (2)	3 (1)	−3 (1)	4 (1)	14 (1)	−12 (1)	11 (1)	−23 (1)	4 (1)	−12 (1)	−1 (1)	7 (2)	−15 (2)	20 (1)	1 (2)	0 (2)
O4	0 (2)	5 (1)	−4 (1)	2 (1)	8 (1)	3 (1)	−3 (1)	−6 (1)	−2 (1)	0 (1)	2 (1)	1 (1)	3 (1)	−1 (1)	1 (1)	3 (1)
	2 (2)	7 (1)	−10 (1)	3 (1)	13 (2)	7 (2)	−2 (2)	−9 (2)	−1 (1)	−2 (1)	−2 (1)	−3 (2)	4 (2)	0 (2)	1 (2)	−2 (2)
C5	6 (2)	−1 (1)	0 (1)	2 (1)	11 (1)	4 (1)	−10 (1)	−20 (1)	1 (1)	9 (1)	−10 (1)	10 (1)	13 (1)	−18 (1)	5 (1)	−4 (1)
	9 (2)	−4 (1)	−4 (1)	9 (1)	15 (1)	6 (1)	−14 (1)	−19 (1)	1 (1)	9 (1)	−11 (1)	16 (1)	12 (2)	−17 (1)	7 (2)	−1 (2)
O5	0 (2)	−2 (1)	−2 (1)	1 (1)	6 (1)	−5 (1)	5 (1)	−7 (1)	−4 (1)	−2 (1)	1 (1)	−2 (1)	−1 (1)	2 (1)	0 (1)	1 (1)
	0 (2)	−3 (1)	−8 (1)	6 (1)	9 (1)	−13 (1)	9 (1)	−4 (1)	−9 (2)	4 (1)	−4 (1)	−3 (2)	1 (2)	1 (1)	−2 (2)	0 (2)
H1	−16 (1)	11 (1)	−6 (1)	5 (1)	6 (1)	−2 (1)	4 (1)	−1 (1)	−6 (2)							
	−20 (1)	12 (1)	−7 (1)	9 (1)	8 (1)	−3 (1)	4 (1)	−7 (1)	−10 (2)							
H3	−21 (1)	−15 (1)	−1 (1)	3 (1)	8 (1)	0 (1)	−10 (1)	2 (1)	−2 (1)							
	−22 (1)	−17 (1)	−3 (1)	5 (1)	10 (1)	−2 (1)	−14 (1)	−6 (1)	−4 (1)							

with invariant core, either *K* shell or Hartree–Fock isolated atom; positional parameters from either X-ray or neutron data; population parameters unconstrained or constrained to 2*mm* molecular symmetry. A conventional high-order refinement was also carried out. Refinements gave $0{\cdot}018 < wR < 0{\cdot}030$.* Results here are for the model in which all nuclear positional parameters and H-atom thermal parameters were given fixed values from neutron diffraction (Tables 1, 2). Anisotropic thermal parameters for the other pseudoatoms were refined. Rigid C, N, O pseudoatoms were given invariant Hartree–Fock isolated atomic cores with X-ray scattering factors from Cromer & Waber (1974) and for H invariant cores were contracted as described by Stewart, Davidson & Simpson (1965). Pseudoatoms were further described by variable electron population parameters applied to deformation terms involving products of a single Slater-type radial and a multipole angular function (Epstein, Ruble & Craven, 1982). Fixed standard values were used for the radial exponents (6·50, 7·37, 8·50, 4·69 Å^{-1} for C, N, O and H respectively). The multipole expansion extended to octapole (quadrupole for H). The monopole population parameters, which are the net charges on each pseudoatom, were constrained to give a zero sum, so that the molecule would be neutral. The model, which included an isotropic extinction parameter [type I crystal, Lorentzian mosaicity; Becker & Coppens (1974)], gave a total of $n = 195$ variables to be determined from $m = 3150$ observations. Refinement converged with $wR = 0{\cdot}020$, $R = 0{\cdot}022$, $S = 1{\cdot}19$† with the parameter values in Tables 2 and 3. A difference Fourier syntheses using all reflections (Fig. 2*a*) showed residual features up to $\pm 0{\cdot}20\,(4)$ e Å^{-3} near the N1 and C5 nuclei. These features were shown to come from the high-resolution data in this refinement, since they became insignificant when only reflections with $(\sin\theta)/\lambda < 0{\cdot}8$ Å^{-1} were included. Residual density maps including all reflections but showing no significant features were obtained by assuming structure models with more variables. In the first such model, all non-H-atom positional parameters were included as variables, giving shifts up to 0·003 Å. However, these shifts might arise from bias in the atomic positions due to sharp features in the static charge density close to the atomic nuclei. In a second model, third-order thermal parameters were introduced for all atoms. This gave only six c_{jkl} values significantly different from zero, the largest being 4·3σ, ($c_{222} = 4 \times 10^{-7}$ for O4). Although the second model is the same as the model adopted for the 298 K refinements (see below), the c_{jkl} values at 123 K are small.* Both models give slightly improved agreement with $wR = 0{\cdot}018$, $R = 0{\cdot}020$, $S = 1{\cdot}13$. However, we accept neither of them because we have no physical basis for preferring one over the other. Neither produces significant changes in the electron population parameters in Table 3.

(iv) *New refinements with* 298 K *data*

The residual electron density at 123 K (Fig. 2*a*) bears little resemblance to the corresponding 298 K map (Fig. 4*b* in CM). In particular, Fig. 2(*a*) shows no features at 123 K which might be attributed to deformations of the static charge density close to the O nuclei. We conclude that such deformations can be neglected at both temperatures. Thus we may assume that sharp features in the residual density at 298 K are

---

* See He (1984) for details, including deformation densities mapped by $(X - X)$ and $(X - N)$ Fourier syntheses.

† $wR = \{\sum(w\Delta^2)/\sum(wF^2_{\rm obs})\}^{1/2}$; $R = (\sum|\Delta|)/[\sum(|F_{\rm obs}|)]$; $S = [\sum(w\Delta^2)/(m - n)]^{1/2}$, $\Delta = |F_{\rm obs}| - |F_{\rm cal}|$.

* See footnote*, p. 273, and He (1984) for tabulated values.

due to anharmonic vibrations which are damped so as to have marginal (if any) significance at 123 K. Accordingly, new refinements were then carried out with the 298 K X-ray and neutron data of CM. The model used was the same as for the 123 K refinements with third-order thermal parameters included for all atoms. The changes from the CM refinements are as follows. For both X-ray and neutron refinements, the Gram–Charlier expression was used for third-order temperature factors c_{jkl} (see Table 4).* In the X-ray refinement, invariant pseudoatom cores were assumed to be neutral Hartree–Fock atoms rather than Clementi two-electron spherical K shells, as in CM. Thus the electron population parameters take on a different meaning, especially the monopole values which give the net excess of negative charge on the pseudoatom instead of the total valence-shell charge. Also, the X-ray refinement included all 3645 reflections with $|F_{\text{obs}}| \geq 0$ using revised weights with $\sigma(F) = \sigma(F^2)^{1/2}/2$ for reflections with $|F_{\text{obs}}|^2 < \sigma(F_{\text{obs}}^2)$, as recommended by Rees (1976). The CM refinements included only 2149 reflections with $|F_{\text{obs}}| > 3\sigma(F_{\text{obs}})$. Nuclear positional and H-atom thermal parameters from the new neutron refinement were used as fixed values in the new X-ray refinement. The new refinements gave convergence with the atomic parameters listed in Tables 1, 2, 3 and 4. For the neutron refinement, $wR(F) = 0{\cdot}022$, $R(F) = 0{\cdot}038$, $S = 1{\cdot}19$ and for the X-ray refinement $wR(F) = 0{\cdot}025$, $R = 0{\cdot}090$, $S = 1{\cdot}21$. The residual electron-density map (Fig. 2*b*) includes only reflections with $|F_{\text{obs}}| > 3\sigma$ to allow direct comparison with the previous maps (Figs. 4*b*, 6*b* in CM). There are similarities presumably because of errors in the data which are common to all refinements. Small differences close to the atom centers are attributed to the changes in the model. The most significant of these [+0·28 (7) e Å^{-3}] is at C5 in Fig. 2(*b*). Sharp dipole features near the O atoms are absent.

Table 4. *Third-order thermal parameters* ($\times 10^7$) *at* 298 K

Only four of the ten c_{jkl} terms per atom are listed, and only those for the O atoms. Except for H1, other c_{jkl} values differ from zero with at most only marginal significance. For H1, $c_{112} = 12\,(5)$, $c_{122} = 14\,(6)$, $c_{113} = 17\,(8)$, $c_{133} = 50\,(15) \times 10^7$. For a complete table, see the deposition footnote. Values are from neutron diffraction (above) and X-ray diffraction (below). Temperature factors have the form

$$T = 1 - \tfrac{4}{3}\pi^3 i \textstyle\sum_j \sum_k \sum_l h_j h_k h_l c_{jkl}.$$

	c_{222}	c_{333}	c_{223}	c_{233}
O2	−12 (8)	28 (40)	16 (8)	−9 (14)
	−8 (3)	49 (14)	15 (4)	18 (7)
O4	25 (9)	−57 (42)	−14 (9)	−46 (15)
	8 (4)	−97 (17)	−32 (5)	−47 (8)
O5	23 (8)	−13 (32)	4 (7)	10 (12)
	20 (3)	−35 (12)	−8 (4)	14 (6)

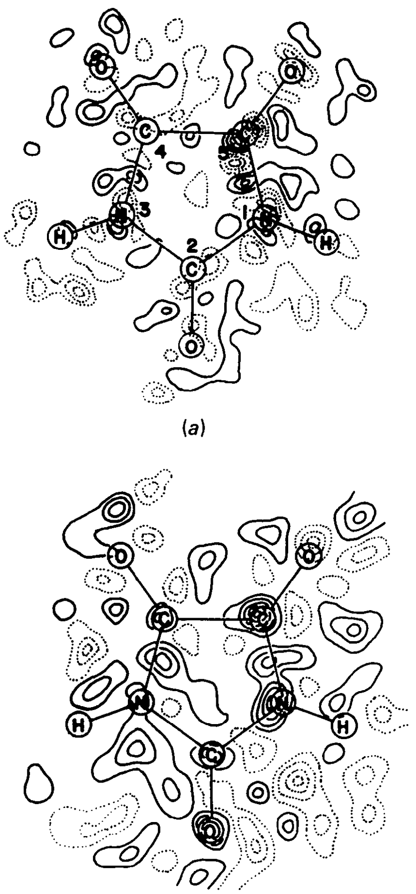

(*a*)

(*b*)

Fig. 2. Fourier syntheses of residual electron density including all reflections $|F| > 3\sigma$. Contours are at intervals of 0·05 e Å^{-3} with the zero contour omitted. Maps follow refinements with X-ray data collected at (*a*) 123 K, (*b*) 298 K.

Discussion

(i) *Atomic thermal vibrations in the harmonic approximation*

The anisotropic thermal parameters of the O, N and C atoms at both temperatures are consistent with the rigid-body model for molecular vibrations (Schomaker & Trueblood, 1968). Thus the least-squares fit of calculated and observed U_{ij} values from neutron diffraction gives $wR = 0{\cdot}029$ and $S = 1{\cdot}23$ for the 123 K data and $wR = 0{\cdot}027$ and $S = 1{\cdot}94$ for the 298 K data. Principal values for the molecular librations are 2·3 (3), 5·1 (6) and 14·5 (8) deg^2 at 123 K

---

* This expression was also supposedly used by CM. However, it was later recognized that the computer program *ORJFLS* (Johnson, 1970) which they used involved an orthogonalization of c_{jkl}. Hence the coefficients given by CM do not correspond to the non-orthogonalized values presently obtained with the *POP* computer programs (Craven & Weber, 1981). This explains the disappointing results when CM used fixed c_{jkl} values from *ORJFLS* in X-ray refinements with *POP*.

and 8 (3), 13 (4) and 35 (6) deg^2 at 298 K, with the maximum libration being about an axis 13° from the approximate molecular twofold symmetry axis.*

As shown in Table 2, there is generally good agreement between values of the anisotropic temperature factors obtained by X-ray and neutron diffraction. The agreement is not as good as in the crystal structure determinations of urea (Swaminathan, Craven, Spackman & Stewart, 1984) and alloxan (Swaminathan, Craven & McMullan, 1985) where it was possible to use fixed thermal parameters from neutron diffraction in the refinement with X-ray data. However, for parabanic acid at 298 K, the agreement is considerably better than was reported by CM. Considering both temperatures, only 7 of the 96 pairs of U_{ij} values differ significantly, the largest [0·0023 (5) Å^2] being $\Delta U_{33} = U^N_{33} - U^X_{33}$ for C4 at 298 K. Although most individual differences are small, they follow trends which indicate the presence of some sytematic error. Thus the average ΔU_{11} for the eight non-H atoms is 0·0006 Å^2 at both 123 and 298 K. Corresponding values are −0·0004 and −0·0005 Å^2 for U_{22} and −0·0011 and +0·0009 Å^2 for U_{33}.

We explored the possibility of systematic error resulting from the neglect of corrections of the Bragg intensities for TDS (thermal diffuse scattering). Such corrections were impractical in this study. However, we must recognize that all U_{ij} values may be underestimated by about 0·0050 Å^2, even at 123 K (Kroon & Vos, 1979), and that significant ΔU_{ij} values may arise from the differences in the correction for X-ray and neutron diffraction (Willis, 1970). Kroon & Vos (1979) point out that TDS has a very small effect on atomic positional parameters, and that the effect on anisotropic thermal parameters is approximately uniform for all atoms. Thus the translational component of any rigid-body motion would be underestimated, but TDS would have little effect on the librational component and hence on the resulting corrections to interatomic distances and angles. We were concerned that the neglect of TDS corrections might affect the electron population parameters in a charge-density study, particularly for the monopole and quadrupole terms which are strongly correlated with the anisotropic thermal parameters. An approximate artificial correction for TDS was introduced for the X-ray data for parabanic acid at 298 K, consisting of a factor $\exp[-8\pi^2U(\sin^2\theta)/\lambda^2]$ with $U = 0{\cdot}0050$ Å^2 applied to all $|F_{\rm obs}|$. This corresponds to the Bragg intensity being reduced by half at $[(\sin\theta)/\lambda]_{\max} = 1{\cdot}0$ Å^{-1}. Least-squares refinement beginning with the atomic parameters from Tables 1 through 4 gave increases in all U_{ij} which were 0·0050 Å^2 within 0·6σ. All changes in p_v and q_j were less than 0·8σ. It is concluded that if there are systematic errors in U_{ij} which are almost uniform for all atoms, the effect on the static charge density in this study will not be serious.

(ii) *Anharmonic vibrations of* O *atoms at* 298 K

Probability density functions (p.d.f.'s) for the atomic thermal vibrations have been calculated from the expression $\rho(u) = \rho_2(u)[1 + \rho_3(u)]$ where $\rho_2(u)$ is the usual Gaussian p.d.f. derived from the anisotropic thermal parameters and $\rho_3(u)$ is a sum of three-dimensional third-order Hermite polynomials. Terms in this sum are weighted by the c_{jkl} coefficients (see Table 4; see also § 5.2.3.1 in Johnson & Levy, 1974). The harmonic Gaussian p.d.f. ρ_2, which is usually represented by a thermal ellipsoid (see Fig. 1), is the major component of the total p.d.f. Thus the maximum of the skewed component $\rho_2\rho_3$ for O4 at 298 K is only 10% of the maximum in the total p.d.f. (Fig. 3). For O2 and O5, the corresponding value is 7%. The accurate determination of c_{jkl} values requires high-resolution data, preferably from neutron diffraction so that the results are unbiased by any features of the static charge density close to the atomic nuclei. For parabanic acid at 298 K, the neutron data are limited to $(\sin\theta)/\lambda <$ 0·76 Å^{-1}, whereas the X-ray data extend to 1·00 Å^{-1}. Higher-resolution neutron data would be desirable. Nevertheless, the skewed components of each O-atom p.d.f. obtained from X-ray and neutron diffraction are in good agreement (Fig. 4). This indicates that the c_{jkl} values have physical significance. From Fig. 4, the observed anharmonicity does not arise from the curvilinear motion of the O atoms resulting from rigid-body molecular librations. Instead, the O-atom vibrations appear to be rectilinear in a direction closely parallel to the approximate molecular twofold symmetry axis (top to bottom in Fig. 2). Along this

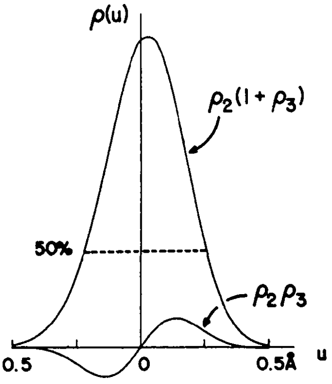

Fig. 3. Profile of the probability density function (p.d.f.) for the thermal vibration of O4 as obtained from X-ray diffraction at 298 K. This is the profile along the line joining the maximum and minimum values shown for O4 in Fig. 4. The curve $\rho_2(1+\rho_3)$ gives the total p.d.f. and $\rho_2\rho_3$ gives the skewed part of the p.d.f. The dashed line is at the level of 50% probability of enclosing the atomic nucleus.

---

* For further details, see the deposition footnote.

direction, there is greater probability for the molecule to be stretched rather than compressed. Such a vibration is favored by the nature of the crystal packing, because during stretching, the O atoms are moving into regions between neighboring molecules. The rectilinear motion of the O atoms at 298 K gives rise to C=O internal vibrations which are a combination of stretching and bending. The rigid-bond test (Harel & Hirshfeld, 1975) using the anisotropic thermal parameters gave mean-square (m.s.) amplitudes of vibration for the O atoms along the C=O bonds only marginally greater than for the C atoms (0·0009 $\AA^2$ for O2; 0·0002 $\AA^2$ for O4 and O5). For these C=O bonds, it appears that the third-order thermal parameters are a more effective indication of non-rigid behavior.

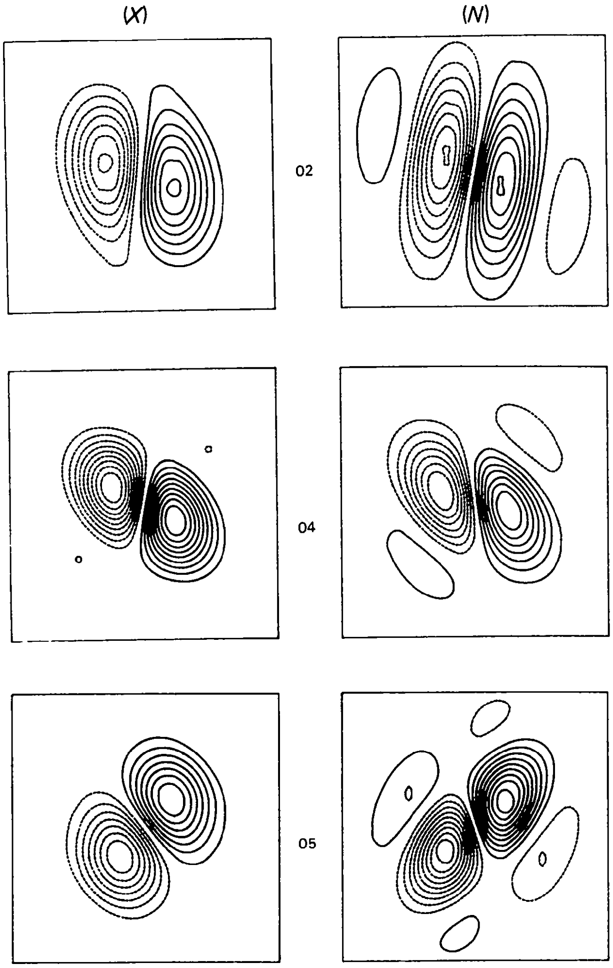

Fig. 4. Sections through the skewed part ($\rho_2\rho_3$) of the p.d.f. at 298 K for the three O atoms. Each section (1 × 1 Å) is in the molecular plane with the O nucleus at the center, with the C=O bond left to right and C at the left (outside each frame). Sections in the left-hand column are from X-ray diffraction (*X*) and those on the right from neutron diffraction (*N*). Contours are at equal intervals (50) with negative contours dashed and the zero contour omitted. In every case, maxima and minima lie within 0·1 Å of the sections shown here.

Of the two H atoms, only H1 has a significant anharmonic motion at 298 K (Table 4). The p.d.f. shows that this corresponds to combined bond stretching and bond bending normal to the plane of the molecule. The distinction between the H atoms may arise because the H bond involving H1 is bent more than the H bond involving H2 [N—H···O angles 161·7 (5) *vs* 171·1 (5)°]. The p.d.f. for H1 is greater on the side of the molecule which leads to a straighter H bond. Thus, when H1 is at the peak of the skewed component of its p.d.f., the N—H···O angle is increased to 173·7°. The rigid-bond test using anisotropic thermal parameters gave m.s. amplitudes of vibration at 298 K along the N—H bonds which are significantly greater for the H than for the N atoms [ΔU = 0·0047 (11), 0·0074 (12) $\AA^2$ for N1—H1 and N3—H3 respectively]. This indicates that, in addition to the anharmonic vibration of H1, there are also harmonic internal stretching vibrations of both N—H bonds. At 123 K, only the harmonic internal stretching remains significant [ΔU = 0·0051 (7), 0·0042 (7) $\AA^2$ for N1—H1 and N3—H3].

(iii) *The molecular structure and intermolecular interactions*

The molecule conforms closely to 2*mm* symmetry at both 123 and 298 K. From neutron diffraction at 123 K, all atoms are nearly coplanar, the largest displacements from the best least-squares plane being −0·009 (1), +0·005 (1) and −0·005 (1) Å for O2, O4 and O5 respectively. At 298 K, none of the atoms is significantly displaced from the best least-squares plane. Bond distances and angles,* except for those involving H atoms, have been corrected for rigid-body librations. The N—H bond distances have been corrected assuming the riding-motion model (Busing & Levy, 1964). In the five-membered ring, there is agreement between pairs of corrected bond lengths and angles which would be related by 2*mm* symmetry. Thus C2—N1 and C2—N3 bond lengths are 1·399 (1) and 1·395 (1) Å, while C5—N1 and C4—N3 bond lengths are 1·360 (1) and 1·362 (1) Å. Corrected C4—O4 and C5—O5 bond lengths agree well [1·214 (1), 1·215 (1) Å] and are slightly longer than C2—O2 [1·206 (1) Å]. The C4—C5 bond length is 1·549 (1) Å. These are all in good agreement with the corrected values at 298 K given by CM and will not be discussed further. The N1—H1 and N3—H3 bond lengths [1·043 (2), 1·047 (2) Å] after the riding-model corrections [0·019, 0·017 Å] are equal within experimental error, both being longer than the librationally corrected values of CM. Corrected bond lengths and angles from the new refinements at 298 K are all in agreement with those of CM, except for the longer N—H bonds [1·055 (7), 1·049 (7) Å]. The

---

* See deposition footnote.

e.s.d.'s in these new values are about three times those of CM due to the increased uncertainty in nuclear mean positions when third-order temperature factors are included in the structure model. The C=O bond lengths corrected only for harmonic molecular librations are 1·206 (3), 1·211 (3) and 1·199 (3) Å for C4—O4, C5—O5 and C2—O2. From Fig. 3, it is estimated that, at the level of the 50% probability envelope, the correction due to anharmonic bond stretching is +0·02 Å.

Uncorrected intermolecular H-bonding distances H1···O4 and H3···O5 are slightly shorter at the lower temperature [1·89 and 1·82 Å at 298 K *vs* 1·86 and 1·81 Å at 123 K]. The corresponding N—H···O angles are 162 and 171° at 298 K *vs* 164 and 170° at 123 K. The unusually short intermolecular O2···C5 distance (see Fig. 2 of CM) which is 2·78 Å at 298 K becomes 2·75 Å at 123 K. On application of the maximum possible correction for the vibrations of the two atoms (Busing & Levy, 1964), these distances become 2·825 (3) Å at 298 K and 2·764 (1) Å at 123 K.

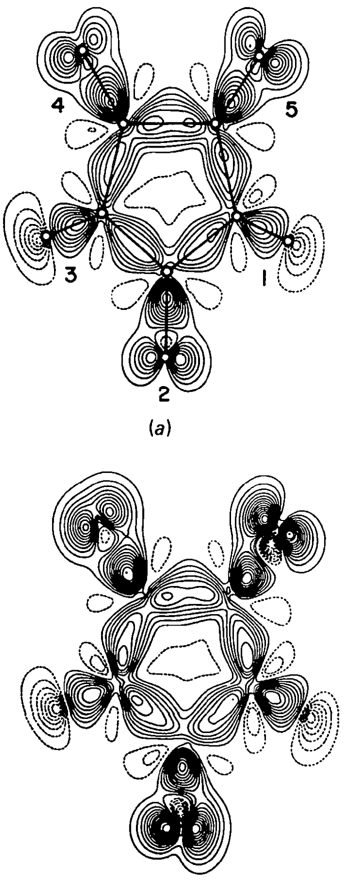

(*a*)

(*b*)

Fig. 5. Deformation charge density in the molecular plane for atoms at rest. Contours at intervals 0·1 e Å^{-3} with zero contour omitted. (*a*) From data collected at 123 K, (*b*) from data collected at 298 K.

(iv) *Comparison of electron population parameters at* 123 K *and* 298 K

The electron population parameters (Table 3) determined at 123 and 298 K are in good overall agreement, although the magnitudes tend to be larger at 298 K. The effect can be seen in the deformation charge density mapped for atoms at rest (Fig. 5) where corresponding features are very similar, but larger in magnitude when derived from the 298 K data, especially at the O atoms. It is believed that the lower-temperature results are more reliable. With increasing temperature, deconvolution of thermal-vibration effects from the static charge density of the O atoms becomes increasingly more difficult because, for the O atoms, the quadrupole terms (q_j, Table 3) are the predominant deformations and these have similar symmetry properties to the anisotropic thermal parameters. It is important to note that the deformation density obtained at 123 and 298 K shows the paired lobes in the lone-pair regions at all three O atoms to lie within the molecular plane. This is in contrast to the results of the earlier 298 K refinement of CM which showed the O4 lobes to be unequally developed and twisted at about 45° from the molecular plane. We attribute the difference primarily to the neglect of the third-order thermal parameters in the CM structure model.

The deformation density (Fig. 5) is also in good agreement with less-accurate results obtained for parabanic acid in the 1:1 complex with thiourea (Weber & Craven, 1987), where the molecules lie in crystallographic mirror planes. Results for the crystal complex come from 298 K X-ray data only. In their Table 2, Weber & Craven (1987) compare electron population parameters for parabanic acid obtained from both crystal structures. Values are transformed to the same molecular Cartesian axial system, making it easier to see that the deformation density for both molecules conforms closely to the 2*mm* symmetry of the isolated molecule. This result is of interest because the refinements we presently report for the parabanic acid crystal structure were carried out with no symmetry constraints imposed.

We conclude that, while the deformation density can be reasonably well deconvoluted from the thermal motion in the crystal at elevated temperatures, nevertheless it is preferable to collect the diffraction data at a temperature as low as possible.

(v) *Molecular electrostatic properties*

Further discussion of electrostatic properties is based on the 123 K results for parabanic acid. The molecular dipole moment $\mu = 2 \cdot 3\,(3)$ D [7·7 (10) × 10^{-30} C m] was calculated from pseudoatom monopole and dipole deformations, following the procedure of Stewart (1972). The direction of μ is not significantly different [10 (18)°] from the direction of the molecular twofold axis. We have found no other experimental value for μ. With respect to the ureide carbonyl group the sense $(-)\rightarrow(+)$ of μ is C2→O2 which is the opposite from that of μ for urea itself {5·4 (5) D [18·0 (16) × 10^{-30} C m]; Spackman, Weber & Craven (1988)}.

Maps of electrostatic potential for parabanic acid (Figs. 6 through 8) are shown for molecules or finite groups of molecules removed from the crystal with all atoms assumed to be at rest. The calculation of the potential makes use of the experimentally determined pseudoatom positional and charge-density parameters (Tables 1 and 3), and is based on a procedure developed by Stewart (1983) and summarized by He (1984; Appendix *A*).

The major features in the potential for a single parabanic acid molecule (Fig. 6) resemble those for alloxan (Swaminathan, Craven & McMullan, 1985; Fig. 6*b*). Most notable are the broad regions of positive potential extending from the H-atom centers. Such regions are characteristic of the electropositive H atoms in N—H and O—H groups, the potential being more contracted around the H atoms in C—H groups, where the H atoms are almost neutral. The difference is well illustrated in electrostatic potential maps for imidazole (Stewart, 1982). In Fig. 6, as in the corresponding map for alloxan, the electronegative region near each carbonyl O atom is very shallow, the minimum value being $-92\ \mathrm{kJ\ mol^{-1}}$ near O4 in parabanic acid. It is of interest to compare the electrostatic potential near the carbonyl groups in parabanic acid and urea. Differences in the polarity of these carbonyl groups are to be expected because the C—O bond lengths are quite different [1·206, 1·214, 1·215 (1) Å for parabanic acid; 1·265 (1) Å for urea (Swaminathan, Craven & McMullan, 1984); values corrected for thermal vibrations]. Indeed, the minimum in electrostatic potential near the urea carbonyl O atom as determined by Stewart (1987) from the charge-density study of Swaminathan, Craven, Spackman & Stewart (1984) is much deeper ($-440\ \mathrm{kJ\ mol^{-1}}$) than the corresponding minima in parabanic acid. Thus the carbonyl O atoms in parabanic acid (and also alloxan) are less electronegative than the carbonyl O atom in urea and should therefore be less effective as H-bond acceptors. This conclusion is of interest because it supports suggestions made by Weber, Ruble, Craven & McMullan (1980) based on their comparisons of observed H-bond distances. Their suggestion was that parabanic acid is more effective as an H-bond donor through its NH groups than as an acceptor through its carbonyl O atoms and that for urea the converse is true. Consequently, they considered the strong H bond (N···O 2·66 Å) with parabanic acid as donor and urea as acceptor to be important for the existence of the 1:1 crystal complex involving these molecules.

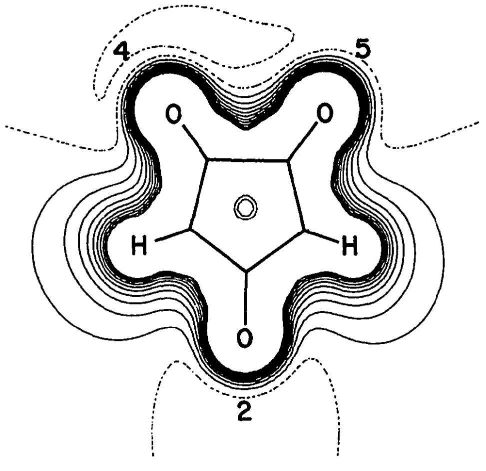

Fig. 6. Total electrostatic potential for a molecule isolated from the crystal. All atoms are at rest. Contours are at intervals 0·05 e Å^{-1} with zero and negative contours as broken lines. A positive probe charge has its minimum potential in negative regions. Because of the contribution from inner electrons and the nucleus, the potential increases sharply to an infinite value at each atom center.

In Fig. 7 is shown the electrostatic potential for the region of H bonding N3—H3···O5 between a pair of

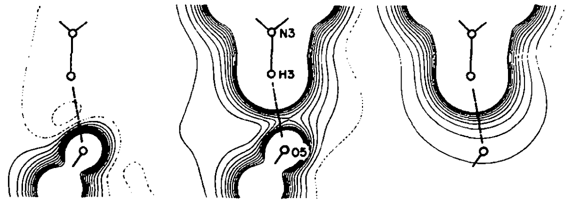

Fig. 7. Total electrostatic potential around the N3—H3···O5 intermolecular hydrogen bond, mapped in the plane of these three atoms. Contours are as in Fig. 6. Contributions to the potential are from complete molecules isolated from the crystal. At left is the potential from the acceptor molecule, at right from the donor and at center from both molecules.

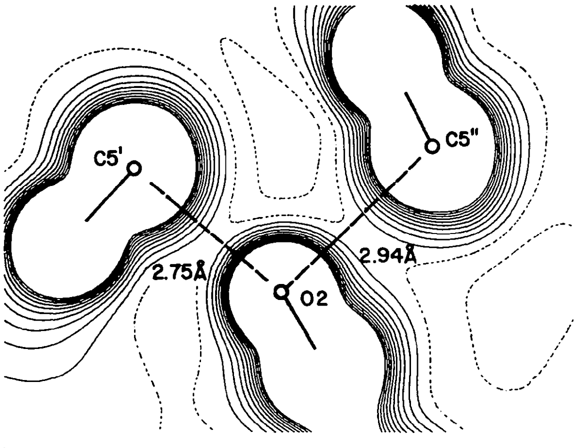

Fig. 8. Total electrostatic potential mapped in the plane C5'···O2···C5'' which contains two short intermolecular distances. Contours are as in Fig. 6. The potential consists of the contributions from three molecules isolated from the crystal.

molecules isolated from the crystal structure of parabanic acid (H3···O5 1·81 Å). Maps for the other H bond (N1—H1···O4) are very similar (He, 1984). For the molecules in Fig. 7, it is seen that the electropositive region from the donor H atom overlaps the electronegative region from the acceptor O atom, forming a weakly electropositive bridge. Similar effects are observed in the bifurcated H-bond region between alloxan molecules (Fig. 8 of Swaminathan, Craven & McMullan, 1985). Such bridges may be a general property of short-range electrostatic molecular interactions, since they also occur in the region of short C···O intermolecular distances in parabanic acid (Fig. 8) and in alloxan (Fig. 8 in Swaminathan, Craven & McMullan, 1985).

(vi) *Energy calculations and crystal stability*

Recently, Spackman (1986, 1987) has developed a simple model for calculating the energies of molecular interactions from diffraction data. The model includes a consistent set of atom–atom potentials with repulsive and dispersive terms derived from electron-gas theory. Spackman, Weber & Craven (1988) have successfully applied this model to calculate H-bonding energies for pairs of molecules taken from the crystal structures of imidazole, 9-methyladenine, cytosine monohydrate and urea. However, in the case of alloxan, it was found that the H bonds were only weakly attractive [$-4{\cdot}2$ kJ mol^{-1}], compared with a single H bond between urea molecules [-25 (8) kJ mol^{-1}]. The H-bond energy remained small ($-16{\cdot}7$ kJ mol^{-1}) when calculated for a pair of double-H-bonded alloxan molecules in an optimized configuration not found in the crystal structure. Thus, it appears that the C···O interactions must be important for molecular cohesion in the crystal structure of alloxan, otherwise it becomes difficult to account for the high crystal density (1·93 g cm^{-3} at 295 K) and the high melting point (529 K, with decomposition). Efforts to modify the Spackman model by omitting the contribution of C···O repulsive and dispersive terms were disappointing, since the interaction energy of two alloxan molecules involving three short C···O distances remained only weakly attractive [-2 (2) kJ mol^{-1}]. Similar results were obtained in energy calculations for pairs of parabanic acid molecules taken from the crystal structure. The electrostatic interaction energy between pairs of molecules which are H bonded is weakly attractive [-7 (3) and -5 (2) kJ mol^{-1} for H3···O5 and H1···O4 respectively]. However, the total energy, including repulsive and dispersive atom–atom terms, becomes zero for both pairs of molecules.

Interaction energies were also calculated for pairs of molecules forming short C···O distances, namely the pair of molecules at (x,y,z) and ($\frac{1}{2}-x$, $\frac{1}{2}+y$, $\frac{1}{2}-z$) for which the O2···C5 and O2···C4 distances are 2·75 and 3·08 Å, and the pair (x,y,z) with ($x, y, -1+z$) with corresponding distances 2·94 and 3·08 Å. The arrangement of these molecules can be seen in Fig. 2 of CM. For both pairs, the total electrostatic interaction energy is repulsive ($+10{\cdot}9$ and $+5{\cdot}4$ kJ mol^{-1} respectively). If the dispersive and repulsive contributions from the close C···O atom pairs are neglected, the total energies become marginally attractive [$-1{\cdot}3$ (4) and -1 (1) kJ mol^{-1} respectively]. As in the case of alloxan, the interaction energies of parabanic acid molecules engaged in H bonding and short C···O distances appear to be too small to account for the considerable stability of these crystals. Thus parabanic acid melts with decomposition at 516 K. Since the Spackman model appears to give a satisfactory approximation for H-bonding energies, we conclude that the energies for the C···O interactions are underestimated. Further efforts are needed in order to understand the nature of these interactions.

We are grateful to Dr R. F. Stewart for providing us with details of his procedure for calculating molecular electrostatic potentials, and also to Drs R. Shiono and J. R. Ruble, Mr Joseph Henriques and Mrs Joan Klinger for technical help. This work was supported by NIH grants GM-22548 and HL-20350. The neutron data collection and some of the computations were carried out at Brookhaven National Laboratory, under contract DE-AC02-76CH00016 with the US Department of Energy.

References

Becker, P. J. & Coppens, P. (1974). *Acta Cryst.* A**30**, 129–147.

Bolton, W. (1964). *Nature (London)*, **201**, 987–989.

Bürgi, H. B., Dunitz, J. D. & Shefter, E. (1974). *Acta Cryst.* B**30**, 1517–1527.

Busing, W. R. & Levy, H. A. (1957). *Acta Cryst.* **10**, 180–182.

Busing, W. R. & Levy, H. A. (1964). *Acta Cryst.* **17**, 142–146.

Busing, W. R., Martin, K. O. & Levy, H. A. (1962). *ORLS*. Report ORNL-TM-305. Oak Ridge National Laboratory, Tennessee, USA.

Craven, B. M. & McMullan, R. K. (1979). *Acta Cryst.* B**35**, 934–945.

Craven, B. M. & Weber, H. P. (1981). *The POP Least-Squares Refinement Procedure*. Tech. Rep., Department of Crystallography, Univ. of Pittsburgh, PA, USA.

Cromer, D. T. & Waber, J. T. (1974). In *International Tables for X-ray Crystallography*, Vol. IV, pp. 71–147. Birmingham: Kynoch Press. (Present distributor D. Reidel, Dordrecht.)

Davies, D. R. & Blum, J. J. (1955). *Acta Cryst.* **8**, 129–136.

Epstein, J., Ruble, J. R. & Craven, B. M. (1982). *Acta Cryst.* B**38**, 140–149.

Harel, M. & Hirshfeld, F. L. (1975). *Acta Cryst.* B**31**, 162–172.

He, X. M. (1984). PhD Dissertation, Univ. of Pittsburgh, PA, USA.

Johnson, C. K. (1970). In *Thermal Neutron Diffraction*, edited by B. T. M. Willis, Ch. 9, pp. 132–159. Oxford Univ. Press.

Johnson, C. K. (1976). *ORTEP*II. Report ORNL-5138. Oak Ridge National Laboratory, Tennessee, USA.

Johnson, C. K. & Levy, H. A. (1974). *International Tables for X-ray Crystallography*, Vol. IV, pp. 311–336. Birmingham: Kynoch Press. (Present distributor D. Reidel, Dordrecht.)

Koester, L. (1977). *Neutron Physics*, edited by G. Hohler, p. 1. Berlin: Springer.

Kroon, P. A. & Vos, A. (1979). *Acta Cryst.* A**35**, 675–684.

Lehmann, M. S. & Larsen, F. K. (1974). *Acta Cryst.* A**30**, 580–584.

McCandlish, L. E., Stout, G. H. & Andrews, L. C. (1975). *Acta Cryst.* A**31**, 245–249.

McMullan, R. K. & Koetzle, T. F. (1979). Unpublished.

Meulenaer, J. de & Tompa, H. (1965). *Acta Cryst.* **19**, 1014–1018.

Nelmes, R. J. (1975). *Acta Cryst.* A**31**, 273–279.

Prout, C. K. & Wallwork, S. C. (1966). *Acta Cryst.* **21**, 449–450.

Pullman, B. (1964). *Acta Cryst.* **17**, 1074–1075.

Rees, B. (1976). *Acta Cryst.* A**32**, 483–488.

Schomaker, V. & Trueblood, K. N. (1968). *Acta Cryst.* B**24**, 63–76.

Spackman, M. A. (1986). *J. Chem. Phys.* **85**, 6579–6586, 6587–6601.

Spackman, M. A. (1987). *J. Phys. Chem.* **91**, 3179–3186.

Spackman, M. A., Weber, H. P. & Craven, B. M. (1988). *J. Am. Chem. Soc.* In the press.

Stewart, R. F. (1972). *J. Chem. Phys.* **57**, 1664–1668.

Stewart, R. F. (1976). *Acta Cryst.* A**32**, 565–574.

Stewart, R. F. (1982). *God. Jugosl. Cent. Kristalogr.* **17**, 1–24.

Stewart, R. F. (1983). Unpublished.

Stewart, R. F. (1987). Unpublished.

Stewart, R. F., Davidson, E. R. & Simpson, W. T. (1965). *J. Chem. Phys.* **42**, 3175–3187.

Swaminathan, S., Craven, B. M. & McMullan, R. K. (1984). *Acta Cryst.* B**40**, 300–306.

Swaminathan, S., Craven, B. M. & McMullan, R. K. (1985). *Acta Cryst.* B**41**, 113–122.

Swaminathan, S., Craven, B. M., Spackman, M. A. & Stewart, R. F. (1984). *Acta Cryst.* B**40**, 398–404.

Templeton, L. K. & Templeton, D. H. (1973). Proc. Am. Crystallogr. Assoc. Meet., Storrs, CT, USA, Abstracts, p. 143.

Weber, H. P. & Craven, B. M. (1987). *Acta Cryst.* B**43**, 202–209.

Weber, H. P., Craven, B. M. & McMullan, R. K. (1983). *Acta Cryst.* B**39**, 360–366.

Weber, H. P., Ruble, J. R., Craven, B. M. & McMullan, R. K. (1980). *Acta Cryst.* B**36**, 1121–1226.

Willis, B. T. M. (1970). *Acta Cryst.* A**26**, 396–401.

Acta Cryst. (1988). B**44**, 281–289

Single-Crystal X-ray Geometries and Electron Density Distributions of Cyclopropane, Bicyclopropyl and Vinylcyclopropane. I. Data Collection, Structure Determination and Conventional Refinements

By Dick Nijveldt and Aafje Vos

Laboratory of Chemical Physics, University of Groningen, Nijenborgh 16, 9747 *AG Groningen, The Netherlands*

(*Received* 21 *November* 1986; *accepted* 9 *December* 1987)

Abstract

Crystal structures of cyclopropane (CP) C_3H_6, bicyclopropyl (BCP) C_6H_{10} and vinylcyclopropane (VCP) C_5H_8 have been determined by accurate single-crystal X-ray measurements at $T \approx 100$ K. In addition to the conventional full-angle refinements [$(\sin\theta)/\lambda < 1{\cdot}15$ Å^{-1} for CP and $< 1{\cdot}22$ Å^{-1} for BCP and VCP], high-order refinements [$(\sin\theta)/\lambda > 0{\cdot}60$ Å^{-1} for CP, $> 0{\cdot}80$ Å^{-1} for BCP and $> 0{\cdot}70$ Å^{-1} for VCP] have been performed to obtain accurate parameters for C atoms. C_3H_6: CP molecules in the crystal approximate the D_{3h} symmetry of the free CP molecule; $M_r = 42{\cdot}08$, orthorhombic, $Cmc2_1$, $a = 7{\cdot}971$ (3), $b = 6{\cdot}575$ (3), $c = 5{\cdot}844$ (2) Å, $V = 306{\cdot}3$ (2) Å^3, $Z = 4$, $D_x = 0{\cdot}913$ Mg m^{-3}, $\lambda(\text{Mo } K\bar{\alpha}) = 0{\cdot}71069$ Å, $\mu = 0{\cdot}540$ cm^{-1}, $F(000) = 96$, $T = 94$ K, $R(F) = 0{\cdot}0328$ and $R_w(F) = 0{\cdot}0280$ for the full-angle refinement on 915 observed independent reflections. C_6H_{10}: The molecules in the crystal have the *trans*-bisected conformation; $M_r = 82{\cdot}15$, orthorhombic, $Cmca$, $a = 8{\cdot}8528$ (7), $b = 5{\cdot}0911$ (3), $c = 11{\cdot}7294$ (13) Å, $V = 528{\cdot}65$ (8) Å^3, $Z = 4$, $D_x = 1{\cdot}033$ Mg m^{-3}, $\lambda(\text{Mo } K\bar{\alpha}) = 0{\cdot}71069$ Å, $\mu = 0{\cdot}616$ cm^{-1}, $F(000) = 184$, $T = 100$ K, $R(F) = 0{\cdot}0389$ and $R_w(F) = 0{\cdot}0414$ for the full-angle refinement on 1817 observed independent reflections. C_5H_8: The molecules in the crystal deviate slightly from the *trans*-bisected conformation; $M_r = 68{\cdot}12$, monoclinic, $P2_1$, $a = 4{\cdot}8792$ (9), $b = 7{\cdot}1617$ (11), $c = 6{\cdot}9230$ (11) Å, $\beta = 105{\cdot}068$ (13)°, $V = 233{\cdot}60$ (7) Å^3, $Z = 2$, $D_x = 0{\cdot}968$ Mg m^{-3}, $\lambda(\text{Mo } K\bar{\alpha}) = 0{\cdot}71069$ Å, $\mu = 0{\cdot}579$ cm^{-1}, $F(000) = 76$, $T = 94$ K, $R(F) = 0{\cdot}0323$ and $R_w(F) = 0{\cdot}0395$ for the full-angle refinement on 3480 observed independent reflections.

1. Introduction

The present study is focused on volatile compounds containing one or two three-membered carbon rings. In addition to the parent compound cyclopropane (CP) C_3H_6, the two derivatives bicyclopropyl (BCP) C_6H_{10} and vinylcyclopropane (VCP) C_5H_8 will be considered (for structural formulae, see Fig. 3). CP is a gas and BCP and VCP are liquids at room temperature.

0108-7681/88/030281-09$03.00